이상 탐지를 이용하여 금성의 UVI 및 LIR 이미지를 사용하여 정지 대기파 탐지

김준성[1], 바르쉬[2], 조세[3], 이연주[3], 차미영[1,2],
[1]한국과학기술원 전산학부, [2]기초과학연구원 데이터사이언스 그룹, [3]기초과학연구원 행성대기그룹
09jkim@kaist.ac.kr, barisbaydargil@ibs.re.kr, josesilva@ibs.re.kr, yeonjoolee@ibs.re.kr, mcha@kaist.ac.kr

Detecting Stationary Atmospheric Waves in Venus with a Self-Supervised Adversarial Model Using Anomaly Detection

Jun Seong Kim[1], Husnu Baris Baydargil[2] , Jose Eduardo Silva[3], Yeon-Joo Lee[3], Meeyoung Cha [1,2]
[1]School of Computing KAIST, [2]Data Science Group, Institute for Basic Science, [3] Planetary Atmospheres Group, Institute for Basic Science

요 약

Atmospheric waves on Venus are formed due to temperature changes, pressure, and other atmospheric variables. These waves can provide important information about the planet's atmospheric dynamics under extreme climate conditions. This paper uses self-supervised anomaly detection models to detect atmospheric waves in two kinds of images: longwave infrared (LIR) and ultraviolet imaging (UVI). Distinct characteristics of LIR and UVI data present new opportunities to analyze the phenomenon. We also evaluate the performance of different models on both data types and find that UVI data is more suitable for detecting atmospheric waves than LIR data. The best-performing model, VQ-GAN, showed an AUC score of 86.53% for LIR data and 90.81% for UVI data.

1. Introduction

Venus is the second planet from the Sun and is similar in size and bulk chemical composition to Earth. However, its atmosphere is drastically different from that of Earth, mainly comprising CO_2 (carbon dioxide) and other minor compounds like SO_2 (sulfur dioxide), which can condense to form clouds at approximately 48-70 km of altitude [7].

Surface-level atmospheric waves on Venus, particularly stationary waves, result from a multitude of factors inherent to the dynamical processes of atmospheric phenomena. By studying these waves, we can learn more about the nature and origin of Venus's atmosphere, which represents extreme climate. Specifically, stationary waves, characterized by their fixed geographic positions over extended periods of time, serve as crucial indicators that hint at the potential correlations between atmospheric dynamics and corresponding topographical features on Venus' surface.

Historically, the identification and analysis of these stationary waves have predominantly relied on manual inspection conducted by experts. However, this methodology has become increasingly impractical, given the sporadic nature of these wave features in existing datasets and the increasing volume of data obtained from current missions, such as the ongoing Akatsuki space probe mission. When it comes to large datasets in various domains, such manual approaches are time-consuming and may lead to human errors and potential oversight of crucial data. With the advance of machine learning methodologies, task-specific designed models may outperform human experts [3].

In response to these challenges, we implement a vector-quantized generative adversarial network (VQ-GAN) [8], a generative model that builds upon our preceding investigation utilizing data collated by the longwave infrared (LIR) camera aboard the Akatsuki space probe. This research extends the scope of our dataset to encompass images captured by the Ultraviolet Imager (UVI) onboard the same spacecraft. When applied to UVI data, our model shows promising results in distinguishing between images that contain or lack stationary wave features when compared to LIR data. Our early findings present a promising alternative to manual detection of stationary wave features, significantly accelerating data analysis by Venus researchers.

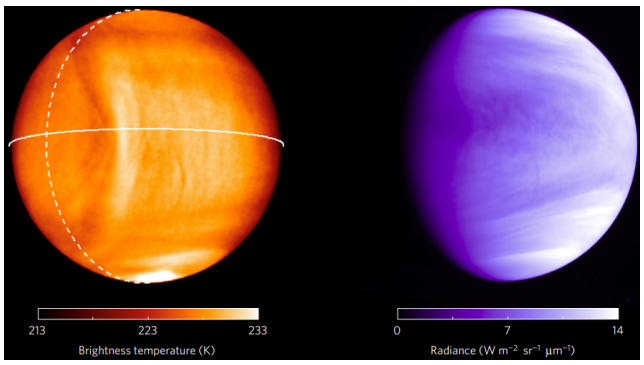

그림 1: LIR (on the left) and UVI (on the right) images of Venus, taken by the Akatsuki space probe on December 7, 2015. A large bow-shaped stationary wave is observed visibly in the left figure.

2. Methodology

2.1 Dataset and Image Preprocessing

Atmospheric data used in this study were taken by the Akatsuki Venus Orbiter in periods December 7th, 2015, and between March 2016 and January 2017, which are the same periods taken in a previous study with confirmed existence of stationary waves [4]. The data comprises LIR and UVI image types and is released publicly by the Japan Aerospace Exploration Agency (JAXA) .

UVI and LIR techniques present unique strengths and weaknesses. LIR uses a longwave infrared spectrum, which is associated with thermal emissions. This is useful for researching temperature mapping, penetration of cloud cover, and access to nightside imaging [2]. On the other hand, LIR may lack clarity and resolution, while indirect inference through temperature variations rather than direct observations may present contradicting informa-

tion. UVI uses the ultraviolet part of the spectrum, ranging from 10nm to 400nm in wavelength. While UVI is helpful for cloud pattern and structure research and SO_2 detection , it has limited penetration into Venus' atmosphere due to thick clouds, which means it cannot provide surface details [1].

Both datasets consist of consecutive Venus images, ranging from a few seconds to several hours. Due to the low-frequency nature of the features in each image, we performed multiple preprocessing steps to highlight the features. The preprocessing pipeline starts with stacking images taken during the same orbiting period of the Akatsuki probe. As stationary waves do not move relative to the sequence of their consecutive images, they are highlighted while the rest of the features are smoothed out.

We employed protocols for both image datasets to ensure the uniformity of the output images. Specifically, the Brightness Temperature, a measure of radiation intensity, was normalized within the LIR dataset, facilitating a more homogenized set of output images. Concurrently, the Lambert Lommel-Seeliger Law was applied to the UVI dataset instead to mitigate the impact of viewing geometry attributable to solar illumination [5]. This process resulted in output images characterized by uniform illumination, thereby removing inconsistencies that might arise due to irregular illumination patterns.

Additionally, we utilized a high-pass filtering technique to accentuate prominent features in the stacked UVI images. This process involved utilizing a Gaussian-smoothed image with a kernel size specified at (25,25), which subsequently yielded images where stationary waves were distinctly visible.

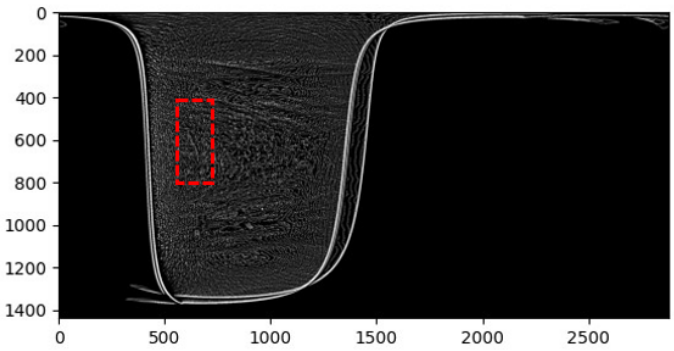

그림 2: UVI image after high-pass filtering taken during early an early period of December 2015.

In processing our model's image data, we divided each image into 72×72 pixel grids and excluded those with over 2,500 black pixels for insufficient information. This procedure yielded roughly 2,000 normal (i.e., images without waves) and 50 stationary wave images in the UVI dataset. Similarly, the LIR dataset comprised around 600 normal and 60 stationary wave images.

2.2 Anomaly Detection Models

In this work, we use three models for anomaly detection, which are VQ-GAN[8], VAE-GAN, and f-AnoGAN [6]. VQ-GAN utilizes vector quantization in its generator. It encodes an input x into a latent representation $E(x)$ and quantizes it using a codebook

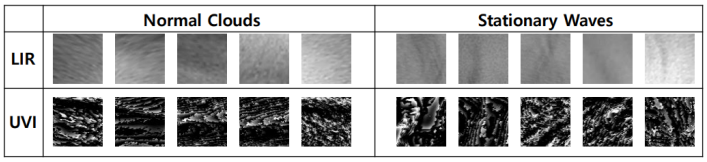

그림 3: Normal Cloud formation (on the left) and stationary wave feature comparison between the LIR and the UVI imaging methodologies.

$C = \{c_1, c_2, \ldots, c_K\}$. The quantized representation z_x is:

$$z_x = \arg\min_{c_i \in C} \|E(x) - c_i\|_2 \tag{1}$$

The generator G then reconstructs the image $\tilde{x} = G(z_x)$. The discriminator D classifies images as real or fake, with the loss:

$$L_D = -(\mathbb{E}[\log D(x)] + \mathbb{E}[\log(1 - D(\tilde{x}))]) \tag{2}$$

VAE-GAN combines Variational Autoencoders (VAE) and GANs. It encodes an input x into a latent space z using an encoder E and decodes it back using a decoder G. The reconstruction loss for the VAE component is:

$$L_{\text{VAE}} = \|x - G(E(x))\|^2 + \text{KL}[E(x)\|N(0, I)] \tag{3}$$

The GAN component involves a discriminator D, which differentiates between real and generated images with a similar loss to traditional GANs.

f-AnoGAN is an efficient anomaly detection model that aims to reduce computational costs while maintaining high performance. The difference between f-AnoGAN and other reconstruction-based models is that there are multiple methods of model training: *izi encoder training* uses residual between real input images and their reconstructed counterparts. izi_f *encoder training* jointly minimizes L_{izi} and L_D by addressing the residual of real and reconstructed images, while L_D focuses on the discriminator's feature residuals. *ziz encoder training* minimizes L_{ziz}, which is based on the residuals in the latent space. We chose the more comprehensive izi_f encoder training in our experiment for better performance.

During the inference, the rest of the normal and all anomaly-designated images are input to the discriminator, where true-positive and false-positive rates are obtained. We calculate the area under the curve (AUC) scores for each model using these results.

To plot the anomaly graph, we compute the anomaly scores using high and low dimensions for each model, for which the weighted anomaly scoring is shown below:

$$S = \lambda \times \text{L1}(x, \tilde{x}) + (1 - \lambda) \times \text{L2}(E(x), E(\tilde{x})) \tag{4}$$

where $\text{L1}(x, \tilde{x})$ is the L1 distance between the input and the reconstructed image, and $\text{L2}(E(x), E(\tilde{x}))$ is the L2 distance between the latent representation of the input and the reconstructed image and λ is the weighting factor, in this experiment, taken as 0.8.

We apply min-max normalization to ensure that the anomaly scores are on a comparable scale. Given a set of anomaly scores

S_i for images $i = \{1, \ldots, N\}$, the normalized score S'_i is:

$$S'_i = \frac{S_i - \min(S)}{\max(S) - \min(S)} \tag{5}$$

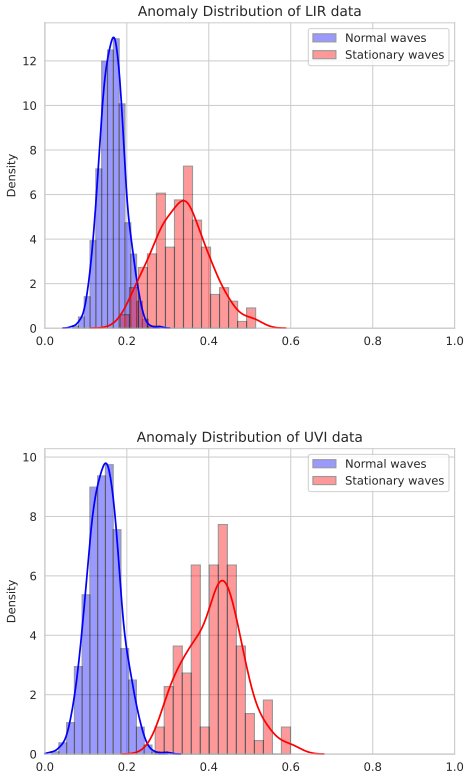

그림 4: Anomaly distributions between normal and stationary waves for the LIR data (top) and the UVI data (bottom) using the VQ-GAN model. It can be seen that anomaly scores for UVI data are higher than the LIR, and at the same time, anomaly scores for normal cloud formations are lower.

3. Results

Although the UVI preprocessing step introduces a heavy amount of noise, it also makes stationary wave features appear more distinctive. On the contrary, LIR preprocessing causes a blurring effect on the image, making the stationary wave features harder to identify. This difference is also reflected in our quantitative and qualitative analyses, where the VQ-GAN achieves 90.81% performance in the AUC score using UVI data, compared to 86.53% using the LIR data. Anomaly detection distribution plots also highlight that the UVI data has much better normal data reconstruction quality and a higher overall anomaly detection rate than the LIR data. VQ-GAN yielded the best performance among the models tested with our data, with UVI data displaying more promising results over LIR applicable for each model.

표 1: AUC comparisons of three anomaly detection models using LIR and UVI datasets.

Model	LIR	UVI
VAE-GAN	78.37%	81.80%
f-AnoGAN	82.72 %	87.39%
VQ-GAN	86.53%	90.81%

4. Conclusion

This work employed three self-supervised models to detect anomalies in the stationary waves of Venus' atmosphere. We compared the performance of LIR and UVI data for this task and found that UVI data was more effective than LIR data in anomaly detection. The best model we used was VQ-GAN, which had the highest AUC scores. In the future, we plan to develop a method to automatically identify and locate stationary features without using manual grids. We also want to study how the atmosphere of Venus changes over time using temporal data.

참고 문헌

[1] *Venus II: Geology, Geophysics, Atmosphere, and Solar Wind Environment*. University of Arizona Press, 1997.

[2] Bruno Bézard, Catherine de Bergh, David Crisp, and Jean-Pierre Maillard. The deep atmosphere of venus revealed by high-resolution nightside spectra. *Nature*, 345(6275):508–511, Jun 1990.

[3] Samuel Dodge and Lina Karam. A study and comparison of human and deep learning recognition performance under visual distortions. In *2017 26th International Conference on Computer Communication and Networks (ICCCN)*, pages 1–7, 2017.

[4] Takehiko Kitahara, Takeshi Imamura, Takao M. Sato, Atsushi Yamazaki, Yeon Joo Lee, Manabu Yamada, Shigeto Watanabe, Makoto Taguchi, Tetsuya Fukuhara, Toru Kouyama, Shin-ya Murakami, George L. Hashimoto, Kazunori Ogohara, Hiroki Kashimura, Takeshi Horinouchi, and Masahiro Takagi. Stationary features at the cloud top of venus observed by ultraviolet imager onboard akatsuki. *Journal of Geophysical Research: Planets*, 124(5):1266–1281, 2019.

[5] Y.J. Lee, T. Imamura, S.E. Schröder, and E. Marcq. Long-term variations of the uv contrast on venus observed by the venus monitoring camera on board venus express. *Icarus*, 253:1–15, 2015.

[6] Thomas Schlegl, Philipp Seeböck, Sebastian M. Waldstein, Georg Langs, and Ursula Schmidt-Erfurth. f-anogan: Fast unsupervised anomaly detection with generative adversarial networks. *Medical Image Analysis*, 54:30–44, 2019.

[7] Dmitrij V. Titov, Nikolay I. Ignatiev, Kevin McGouldrick, Valérie Wilquet, and Colin F. Wilson. Clouds and hazes of venus. *Space Science Reviews*, 214(8):126, Nov 2018.

[8] Jiahui Yu, Xin Li, Jing Yu Koh, Han Zhang, Ruoming Pang, James Qin, Alexander Ku, Yuanzhong Xu, Jason Baldridge, and Yonghui Wu. Vector-quantized image modeling with improved VQGAN. In *The Tenth International Conference on Learning Representations (ICLR)*. OpenReview.net, 2022.